

$M2$ transitions between the $1f_{7/2}$ and the $1d_{3/2}$ orbit*

J. Keinonen,[†] R. Rascher, M. Uhrmacher, N. Wüst,[‡] and K. P. Lieb
Institut für Kernphysik, Universität zu Köln, Köln, Germany
 (Received 11 March 1976)

States in $^{35,36}\text{Cl}$, ^{40}K , and ^{41}Ca decaying predominantly by $M2$ transitions were excited in oxygen induced fusion-evaporation reactions. Their lifetimes were determined by means of the recoil distance Doppler shift technique. A survey on $M2$ transitions between the $1f_{7/2}$ and the $1d_{3/2}$ shell in $33 \leq A \leq 47$ nuclei is presented and the retardations of these transition strengths are discussed. A correlation between the reduced $M2$ matrix elements and the transition energies has been established.

NUCLEAR REACTIONS ^{25}Mg , $^{27}\text{Al}(^{16}\text{O}, xy\gamma)$, 30–50 MeV; measured E_γ , I_γ , recoil distance Doppler shift. ^{36}Cl deduced branching ratio, $^{35,36}\text{Cl}$, ^{40}K , ^{41}Ca deduced $T_{1/2}$. Enriched target.

I. INTRODUCTION

Low lying isomeric states in nuclei near ^{40}Ca very often decay by stretched magnetic quadrupole transitions. Electronic timing techniques have been used to measure their mean lives in the range between a few nsec and 628 μsec in the case of the 150 keV $\frac{3}{2}^+$ state in ^{43}Sc .^{1,2} Recently, a group of $M2$ transitions with γ -ray energies around 3 MeV has been identified in reactions induced by α particles and heavy ions.¹ Lifetimes of typically 30–100 psec have been determined with the recoil distance Doppler shift method by exploiting the large recoil velocity of the final nuclei ($v/c = 2\text{--}3\%$) produced in fusion-evaporation reactions with a 30–50 MeV oxygen beam.

An intuitive interpretation of such transitions relies on the nuclear shell model and is connected with the deexcitation of one nucleon from the $1f_{7/2}$ to the $1d_{3/2}$ orbit. Single-nucleon transfer reactions^{3,4} in the upper half of the sd shell have, indeed, revealed large $f_{7/2}$ single-particle components in the wave functions of the lowest $\frac{7}{2}^-$ states and their analogs, the spectroscopic factor being $S=0.54$ on the average. Similarly, pick-up reactions to the lowest $\frac{3}{2}^+$ states in the odd K, Ca, and Sc isotopes⁵ indicated sizable $d_{3/2}$ single-hole components. Moreover, the lowest 7^+ states in the odd-odd P, Cl, and K isotopes have been found to be strongly populated in (α, d) reactions with two aligned $f_{7/2}$ nucleons being transferred⁶ to the ground states of even-even Si, S, and Ar nuclei, respectively.

In spite of the predominant $(d_{3/2}^n f_{7/2}^m)$ particle-hole nature of these levels, a rather systematic hindrance of the $M2$ transitions by a factor of 5–300 with respect to the $1f_{7/2} \rightarrow 1d_{3/2}$ single-particle

estimate has been observed.^{1,7,8} Similar retardations have been found for the unique first-forbidden $1f_{7/2} \rightarrow 1d_{3/2}$ β transitions.⁹ This is not unexpected, as these γ - and β -matrix elements involve similar transition operators.

For $A=39, 41$ and the Sc isotopes, Kurath and Lawson⁷ and Macfarlane⁸ discussed the $M2$ transitions in terms of the Bansal-French-Zamick model^{10,11} and the strong-coupling model, showing that isospin effects and/or quadrupole deformation can account for the observed inhibitions. More extensive shell model calculations,^{12,13} both within the highly truncated $\{d_{3/2}f_{7/2}\}$ and within the full $\{2s1d1f2p\}$ model space, have been performed by several authors. As to the β decays, Towner, Warburton, and Garvey⁹ have demonstrated that the repulsive $T=1$ interaction between a $1f_{7/2}$ particle and a $1d_{3/2}$ hole introduces a coherent decrease of the β -matrix element. As this inhibition turned out to be rather independent of the nucleus, it has been customary to renormalize the free nucleon coupling constant. The same conclusion has been drawn by Ejiri and coworkers¹⁴ in the case of $1h_{11/2} - 1g_{7/2}$ single-nucleon $M2$ transitions. These authors found that the isovector and isoscalar components of the $M2$ matrix element are inhibited by a factor of about 4 with respect to the single-particle estimate.

The motivation for undertaking the present study was twofold: We first wanted to measure the γ decay of the 5.31 MeV 7^+ state in ^{36}Cl .⁶ In the context of this paper, we were most interested in the $M2$ strength of the 5.31–2.52 MeV $7^+ \rightarrow 5^-$ transition. It should be pointed out that ^{36}Cl offers the rare feature of two successive stretched $M2$ transitions, as the 2.52 MeV 5^- state decays via $M2$ to the 0.79 MeV 3^+ state. Furthermore, the life-

times of the 2.54 MeV state in ^{40}K [$\tau = 1.5 \pm 0.3$ nsec (Ref. 1)] and the 2.01 MeV state in ^{41}Ca [$\tau = 0.8 \pm 0.2$ nsec (Ref. 15)] lie on the borderline between electronic timing and the plunger tech-

nique, and a remeasurement of these lifetimes with improved accuracy seemed desirable.

The second aim of this paper was to present a survey of experimental M2 strengths gathered in

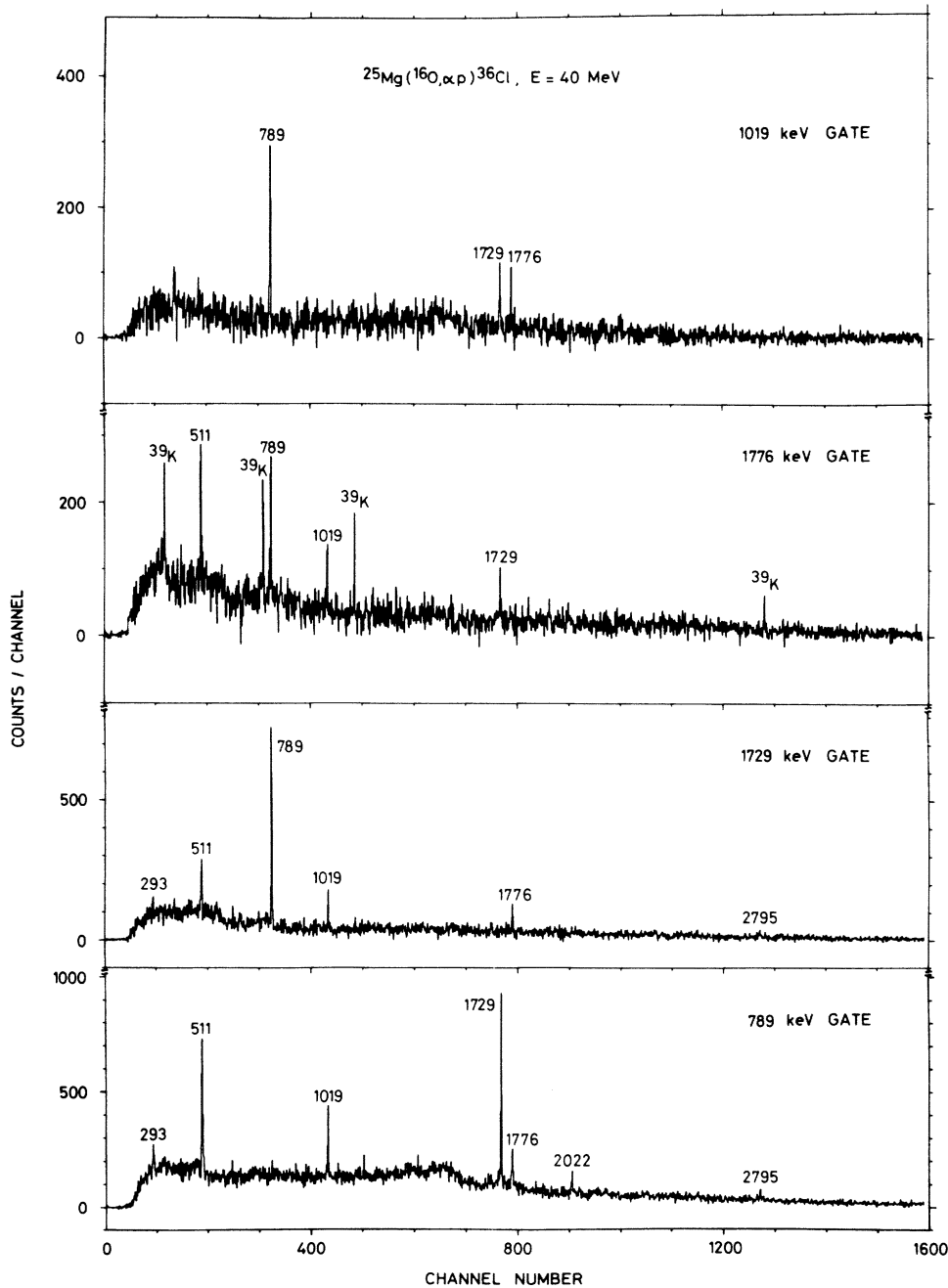


FIG. 1. γ - γ coincidence spectra taken in the reaction $^{25}\text{Mg}(^{16}\text{O}, \alpha p)^{36}\text{Cl}$ at 40 MeV. The ^{39}K lines in the spectrum of the 1776 keV gate are concurrently produced in the reaction $^{25}\text{Mg}(^{16}\text{O}, pn)$ and associated with the decays of the 6.47 and 5.34 MeV states in ^{39}K (see Ref. 24).

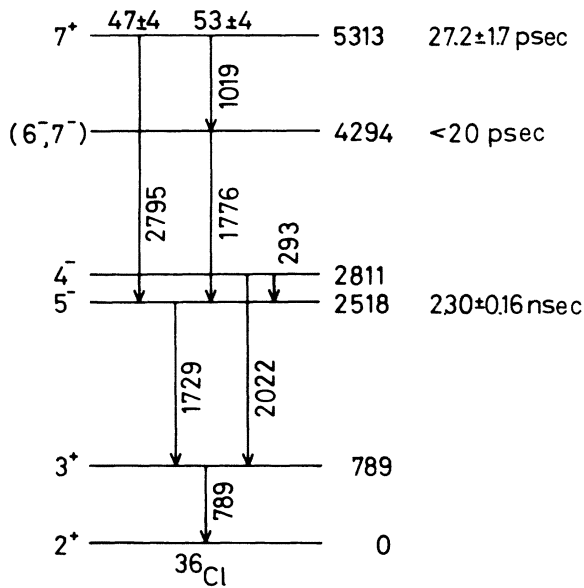


FIG. 2. Decay of high spin states in ^{36}Cl as found from the present study and Ref. 17.

recent years for nuclei around ^{40}Ca and to discuss their retardations with respect to the single-particle estimate.

II. EXPERIMENTAL PROCEDURE AND RESULTS

A. Decay of the 5.31 MeV state in ^{36}Cl

The decays of high spin states in ^{36}Cl were established from a study of the reaction $^{25}\text{Mg}(^{16}\text{O}, \alpha p)$. A $300 \mu\text{g}/\text{cm}^2$ enriched ^{25}Mg target (99.2%) evaporated onto a Ta backing was used in which the beam and the recoiling nuclei were stopped. At 40 MeV oxygen energy, γ - γ coincidences were taken in two true coaxial Ge(Li) detectors of 45 cm^3 volume positioned at 90° on opposite sides of the beam, recorded in an event-by-event mode and stored on magnetic tape. Details of the data storage procedure and analysis have been given previously.¹⁶ Some coincidence spectra are shown in Fig. 1 and the transitions were ordered into the level scheme presented in Fig. 2. In addition to the known states up to and including the 2811 keV state,^{1,17} three transitions of 1019, 1776, and 2795 keV have been observed. Their relative intensities were determined at a beam energy of 35 MeV from efficiency calibrated singles γ -ray spectra and angular distributions. The transitions were attributed to the decay of states at 5313 ± 1 and 4294 ± 1 keV excitation energy.

Spin and parity assignments of the 4.29 MeV level are based on the following arguments: The assignment $I^\pi(5.31) = 7^+$ was derived by Sherr

*et al.*⁶ from the fact that this state is most strongly populated in the two-nucleon transfer reaction $^{34}\text{S}(\alpha, d)$ and that the angular distribution is typical for the simultaneous transfer of an $f_{7/2}$ proton and an $f_{7/2}$ neutron with maximum alignment ($J=7$, $T=0$). From γ -ray angular distribution and polarization data taken in the reaction $^{33}\text{S}(\alpha, p)$, Nolan *et al.*¹⁷ determined $I^\pi(2.52) = 5^-$ and $I^\pi(2.81) = 4^-$, respectively. Likewise, Olness *et al.*¹⁸ measured γ -ray angular distributions and linear polarizations in the reactions $^{24}\text{Mg}(^{18}\text{O}, \alpha pn)^{36}\text{Cl}$ and $^{27}\text{Al}(^{14}\text{N}, \alpha p)^{36}\text{Cl}$, without, however, constructing a level scheme of ^{36}Cl . For the 1019 keV transition they found pure E1 character. The linear polarization of the 2795 keV transition suggests a dominant M2 component, although the rather large error bars do not allow one to assess the magnitude of a possible E3 admixture. No polarization has been measured for the 1776 keV transition. However, its angular distribution and the limit $\tau < 20$ psec on the lifetime of the 4.29 MeV state (see below) require this transition to be either E2 or mixed E2/M1. This rules out all assignments except $I^\pi(4.29) = 6^-$ or 7^- . At 35 MeV beam energy, the 5.31 MeV state is about twice as strongly populated as the 4.29 MeV state. This indicates that the spin of the 5.31 MeV state is higher than that of the 4.29 MeV state, for which $I^\pi = 6^-$ is thus the most probable spin assignment.

B. Lifetime measurements in $^{35,36}\text{Cl}$, ^{40}K , and ^{41}Ca

The lifetimes of the 2.52 MeV 5^- and 5.31 MeV 7^+ states in ^{36}Cl as well as those of three other states in ^{35}Cl , ^{40}K , and ^{41}Ca were determined by means of the recoil distance Doppler shift method. As shown in Table I, these nuclei were produced in the bombardment of ^{25}Mg and ^{27}Al targets with a 30–50 MeV ^{16}O beam. At recoil velocities of $v/c = 2\text{--}3\%$, a clear separation of the energies of the Doppler shifted and unshifted components of each line was achieved.

The plunger device used has been described previously.¹⁹ The flight distance D extended between the stretched movable target and a $10 \mu\text{m}$ thick Ta stopper foil. The stopper was kept in a fixed position in order to avoid solid angle corrections for the count rate in the γ -ray detector when changing the flight distance D . The accuracy of the distance setting was typically $\pm 2 \mu\text{m}$. For $D < 200 \mu\text{m}$, a higher precision of $\pm 1 \mu\text{m}$ was reached by monitoring the capacity of the target-stopper system.²⁰ A previous check of the plunger apparatus had demonstrated that lifetimes as small as 0.6 psec can be measured with our device.²¹ Singles γ -ray spectra were taken at 0° , 30° , or 55° to the beam in 45–85 cm^3 Ge(Li) detectors at flight distances between 1 μm and 8 mm. For each transition con-

TABLE I. Recoil distance measurements.

(a) Experimental conditions					
Nucleus	Reaction	Beam energy (MeV)	Angle θ_γ	Target thickness ($\mu\text{g}/\text{cm}^2$)	v/c (%)
^{35}Cl	$^{25}\text{Mg}(^{16}\text{O}, \alpha pn)$	43	30	150 ^a	2.72 ± 0.08
		50	30		2.95 ± 0.02
^{36}Cl	$^{25}\text{Mg}(^{16}\text{O}, \alpha p)$	43	30	150 ^a	2.72 ± 0.08
		50	30		2.95 ± 0.02
^{40}K	$^{27}\text{Al}(^{16}\text{O}, 2pn)$	32.5	0	270 ^b	2.19 ± 0.03
		35	55	430 ^b	2.13 ± 0.01
		44	0	270 ^a	2.41 ± 0.04
^{41}Ca	$^{27}\text{Al}(^{16}\text{O}, pn)$	30	55	430 ^b	1.90 ± 0.02

(b) Results				
Nucleus	State E_x (keV)	Present	Lifetime τ (psec)	
			Previous	Adopted
^{35}Cl	3162	41.7 ± 1.7	60 ± 7 ^c	43 ± 2
			37 ± 4 ^d	
			53 ± 6 ^e	
			42 ± 3 ^f	
			42 ± 2 ^g	
			43 ± 10 ^h	
^{36}Cl	5313 2518	27.2 ± 1.7 2300 ± 160	...	27.2 ± 1.7 2330 ± 120
			2360 ± 160 ⁱ	
^{40}K	2543	1580 ± 110	1500 ± 300 ^j	1560 ± 100
^{41}Ca	2011	670 ± 70	800 ± 200 ^k	700 ± 70

^a Target evaporated onto 1.5 μm Au backing.

^b Target self-supporting.

^c Reference 36.

^d Reference 37.

^e Reference 38.

^f Reference 39.

^g Reference 29.

^h Reference 25.

ⁱ Reference 17.

^j Reference 1.

^k Reference 15.

sidered, the intensity of the unshifted component $R(D)$ was evaluated and normalized with respect to the intensity of the 301–0 keV transition produced after Coulomb excitation in the Ta stopper, which is proportional to the charge collected.

The analysis of the $R(D)$ curves, some of which are displayed in Figs. 3–5, followed the method described by Lieb *et al.*¹⁹ Usually, delayed feeding due to higher discrete long lived states offers the most serious problems in the analysis. This was, fortunately, not the case in the present experiment: No such feeding was observed for the 5.31 MeV state in ^{36}Cl , the 2.54 MeV state in ^{40}K , and the 2.01 MeV state in ^{41}Ca , and the corresponding $R(D)$ curves are thus pure exponential functions. As to the 3.61 MeV state in ^{35}Cl , the only candidate for delayed feeding is the 6.09 MeV $\frac{13}{2}^-$ state [$\tau = 9.3 \pm 0.8$ psec (Ref. 22)], whose population,

however, is weak at these beam energies. Furthermore, the average time delay introduced by the “continuous” γ -ray cascade feeding the discrete levels (the so called “feeding time”) is much smaller in these light nuclei than the lifetimes 25 psec $< \tau < 1.5$ nsec studied here. No correction for hyperfine deorientation during recoil in vacuum was applied. This effect has been investigated by Rascher *et al.*²³ for high spin states in ^{38}Ar , ^{41}K , and ^{41}Ca nuclei recoiling at $v/c \approx 2\%$. The long deorientation time constants of >1 nsec observed in their measurement had been attributed to the high nuclear and low electronic angular momenta involved. The same arguments apply also for the present measurement, except for the 2.01 MeV state in ^{41}Ca , whose low spin $I = \frac{3}{2}$ eventually would make it vulnerable to deorientation effects. Therefore, this $R(D)$ curve was measured at $\theta_\gamma = 55^\circ$,

where $P_2(\cos\theta_\gamma)=0$ and no time dependent attenuation of the angular distribution occurs.

In the decay curve of the 1776 keV line in ^{36}Cl , we observed a short component corresponding to a lifetime of about 10 psec [see the first three data points of the $R(D)$ curve displayed in Fig. 4.] However, this line was not completely resolved from the 1773 keV transition in ^{39}K which is concurrently formed in the reaction $^{25}\text{Mg}(^{16}\text{O},pn)$ and which has an effective decay constant of 12 psec (Ref. 24); we are thus able to give only an upper limit of $\tau < 20$ psec for the lifetime of the 4.29 MeV state in ^{36}Cl .

The measured lifetimes are summarized in Table I(b). The agreement of our data with previous measurements, frequently less precise, is good. In the case of the 2.52 MeV state in ^{36}Cl , we find excellent agreement with the figure reported by Nolan *et al.*¹⁷ As to the 2.01 MeV state in ^{41}Ca , the lifetime $\tau = 670 \pm 70$ psec determined in the present recoil distance experiment is smaller than, although still compatible with, the value $\tau = 800 \pm 200$ psec derived from electronic timing.¹⁵ We finally note that Merdinger and Dehnhardt²⁵ measured $\tau = 26 \pm 5$ psec for the decay of a 2795 keV line, which they tentatively associated with the 2.795 MeV $\frac{7}{2}^-$ state in ^{39}Ca . As the lifetime of this latter state in ^{39}Ca has been determined subsequently to be $\tau = 90 \pm 24$ psec (Ref. 26) and a large number of residual nuclei are produced in this type of heavy ion fusion reaction,²⁷ we suggest that the shorter lifetime should be attributed to the 5.31 MeV 7^+ state in ^{36}Cl , which we find, indeed, to decay with a time constant of $\tau = 27.2 \pm 1.7$ psec by a 2795 keV branch (see Figs. 2 and 4).

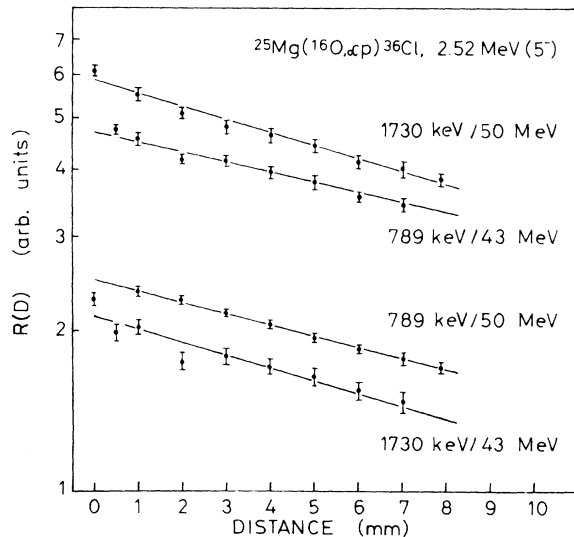


FIG. 3. Recoil distance data for the decay of the 2.52 MeV state in ^{36}Cl .

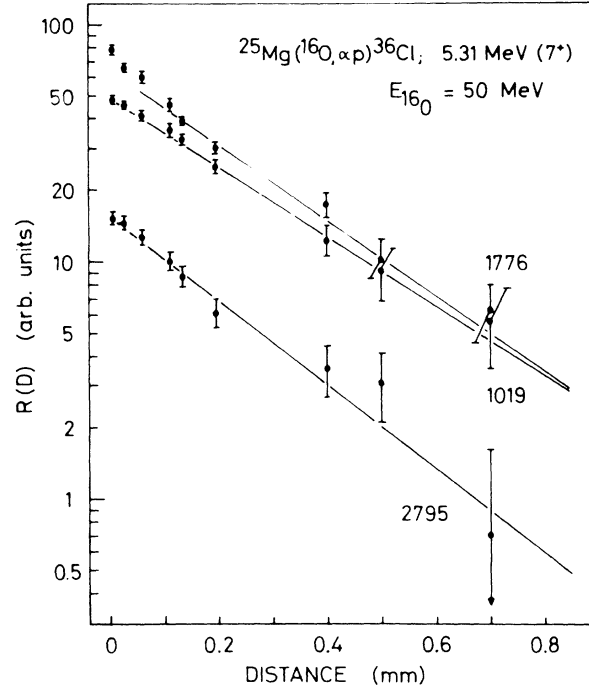


FIG. 4. $R(D)$ functions for transitions depopulating the 5.31 MeV state in ^{36}Cl .

III. DISCUSSION

A. Survey of experimental data

The experimental reduced transition probabilities of all known stretched $M2$ transitions in the region $33 \leq A \leq 47$ were calculated using

$$B(M2)_{\text{exp}} = \frac{73.19}{\tau} \frac{b}{E_\gamma^5(1+\delta^2)} \mu_0^2 \text{fm}^2. \quad (1)$$

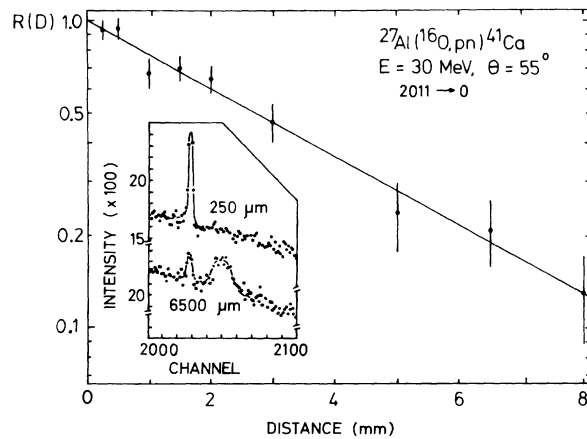


FIG. 5. Decay function of the 2.01 MeV state in ^{41}Ca . The insert shows samples of the recoil distance data exhibiting the Doppler shifted and unshifted peaks of the $2.01 \rightarrow 0$ MeV transition.

Here, τ (in nsec) denotes the mean lifetime of the level, E_γ (in MeV) the transition energy, b the branching ratio, δ the $E3/M2$ mixing ratio, and μ_0 the nuclear magneton. The results obtained are summarized in Table II. For all cases where mixing ratios have been measured, they were found to be of the order $|\delta| \approx 0.15$. By inferring $\delta = 0$ in the other cases with unknown δ , we possibly overestimate $B(M2)_{\text{exp}}$ by about 2%. The reduced transition probabilities range between $0.7 \mu_0^2 \text{ fm}^2$ and $7.4 \mu_0^2 \text{ fm}^2$, clustering around $3.0 \mu_0^2 \text{ fm}^2$. As to the 3.11 MeV state in ^{37}Cl , we adopted the lifetimes measured by Cooke *et al.*²⁸ and by Brandolini *et al.*²⁹

The experimental $B(M2)$ values and reduced matrix elements $\mathfrak{M} = \langle \|M2\| \rangle$ obtained from $B(M2)$

$= \langle \|M2\| \rangle^2 / (2I+1)$ are plotted in Fig. 6 versus the transition energy E_γ . It is interesting to note that there seems to exist a correlation between $|\mathfrak{M}|$ and the transition energy as long as one excludes the two $7^+ \rightarrow 5^-$ transitions in ^{36}Cl and ^{40}K . The reduced matrix element increases from about $|\mathfrak{M}| = 2 \mu_0 \text{ fm}$ at $E_\gamma = 0.15 \text{ MeV}$ to $|\mathfrak{M}| \approx 6 \mu_0 \text{ fm}$ at $E_\gamma = 3.3 \text{ MeV}$. The origin of this correlation is not now known.

B. Single-particle estimates

The experimental $B(M2)$ values have been compared first with the single-particle estimate B_{sp} . In the case of a stretched $f_{7/2} \rightarrow d_{3/2}$ $M2$ transition, $B(M2)$ is given by³⁰

TABLE II. Summary of $M2$ transitions for nuclei with $33 \leq A \leq 47$. (All numbers for which no reference is given have been taken from Ref. 1).

Nucleus	$E I$ initial state	$E' I'$ final state	τ (psec unless noted otherwise)	Branching ratio b (%)	$E3/M2$ mixing ratio δ	$B(M2)$ ($\mu_0^2 \text{ fm}^2$)	$B_{\text{sp}}/B_{\text{exp}}$
^{33}S	2934, $\frac{7}{2}^-$	$0, \frac{3}{2}^+$	41 ± 2	43 ± 4	$+0.13 \pm 0.03$	3.47 ± 0.38	14.3 ± 1.6
^{35}S	1992, $\frac{7}{2}^-$	$0, \frac{3}{2}^+$	1470 ± 70	100		1.58 ± 0.08	33 ± 2
^{35}Cl	3162, $\frac{7}{2}^-$	$0, \frac{3}{2}^+$	43 ± 2^k	90 ± 1	-0.16 ± 0.02	4.73 ± 0.24	18.1 ± 0.9
^{36}Cl	5313, 7^+ 2518, 5^-	2518, 5^- 789, 3^+	27.2 ± 1.7^k 2330 ± 120^k	47 ± 4^k 96 ± 1^l	$+0.11 \pm 0.01^l$	7.4 ± 0.8 1.90 ± 0.10	
^{37}Cl	3105, $\frac{7}{2}^-$	$0, \frac{3}{2}^+$	23 ± 3^b	100	-0.18 ± 0.01^a	10.6 ± 1.4	8.4 ± 1.0
^{37}Ar	1611, $\frac{7}{2}^-$	$0, \frac{3}{2}^+$	6380 ± 150^c	100	$+0.12 \pm 0.02$	1.04 ± 0.02	51.6 ± 1.0
^{37}K	1379, $\frac{7}{2}^-$	$0, \frac{3}{2}^+$	$15\,000 \pm 700$	100		0.98 ± 0.05	90 ± 5
^{39}Ar	1517, $\frac{3}{2}^+$	$0, \frac{7}{2}^-$	1370 ± 70	45 ± 5		3.00 ± 0.37	37 ± 5
^{39}K	2814, $\frac{7}{2}^-$	$0, \frac{3}{2}^+$	68 ± 4^d	100	-0.14 ± 0.02^h	5.98 ± 0.44	15.4 ± 1.1
^{39}Ca	2795, $\frac{7}{2}^-$	$0, \frac{3}{2}^+$	90 ± 24^e	100	$+0.13 \pm 0.07$	4.7 ± 1.0	11.8 ± 2.5
^{40}K	2543, 7^+	892, 5^-	1560 ± 100^k	88 ± 2^i	0.00 ± 0.03^i	3.37 ± 0.25	
^{41}K	1294, $\frac{7}{2}^-$	$0, \frac{3}{2}^+$	$10\,400 \pm 300$	100		1.94 ± 0.06	49 ± 2
^{41}Ca	2011, $\frac{3}{2}^+$ 3370, $\frac{11}{2}^+$	$0, \frac{7}{2}^-$ $0, \frac{7}{2}^-$	700 ± 70^k 29 ± 2^f	100 39 ± 2^f		3.17 ± 0.32 2.26 ± 0.19	36 ± 4
^{43}K	738, $\frac{7}{2}^-$	$0, \frac{3}{2}^+$	$(205 \pm 10) \text{ nsec}^g$			1.63 ± 0.08	60 ± 3
^{43}Ca	990, $\frac{3}{2}^+$	$0, \frac{7}{2}^-$	70 ± 10	0.28 ± 0.03		3.1 ± 0.4	19.1 ± 2.5
^{43}Sc	152, $\frac{3}{2}^+$	$0, \frac{7}{2}^-$	$(628 \pm 10) \mu\text{sec}$	100		1.41 ± 0.02	133 ± 2
^{45}Sc	13, $\frac{3}{2}^+$	$0, \frac{7}{2}^-$	$(440 \pm 25) \text{ msec}$			1.36 ± 0.06	148 ± 7
^{47}Sc	760, $\frac{3}{2}^+$	$0, \frac{7}{2}^-$	$(400 \pm 60) \text{ nsec}$			0.72 ± 0.11	289 ± 44

^a Reference 46.

^b References 28 and 29.

^c Reference 40.

^d References 24 and 41.

^e Reference 26.

^f References 19 and 42.

^g Reference 43.

^h Reference 44.

ⁱ Reference 45.

^k Table I(b) and/or present work.

^l Reference 17.

$$\begin{aligned}
B_{s.p.}(M2, \frac{3}{2} \rightarrow \frac{7}{2}) &= 2B_{s.p.}(M2, \frac{7}{2} \rightarrow \frac{3}{2}) \\
&= \frac{5}{\pi} \mu_0^2 \langle r \rangle^2 (\frac{3}{2} \frac{1}{2} 20 | \frac{7}{2} \frac{1}{2})^2 (g_s - \frac{2}{3} g_1)^2 \\
&= 0.819 \mu_0^2 \langle r \rangle^2 (g_s - \frac{2}{3} g_1)^2. \quad (2a)
\end{aligned}$$

This corresponds to a reduced matrix element of

$$\mathfrak{M}_{s.p.} \equiv \langle \frac{7}{2} || M2 || \frac{3}{2} \rangle = +1.81 \mu_0 \langle r \rangle (g_s - \frac{2}{3} g_1). \quad (2b)$$

Approximating the radial matrix element by $\langle r \rangle = 0.75 r_0 A^{1/3} \approx 3.1$ fm for $A = 40$ and $r_0 = 1.2$ fm,³⁰ one obtains $\mathfrak{M}_{s.p.} \approx 27 \mu_0$ fm for a $\frac{7}{2} \rightarrow \frac{3}{2}$ single-proton transition and $\mathfrak{M}_{s.p.} \approx -21 \mu_0$ fm for the corresponding single-neutron transition. It follows from Fig. 6 that the experimental reduced matrix elements are retarded by a factor of 3 to 12 relative to these single-particle estimates.

For all $\frac{7}{2}^- \rightarrow \frac{3}{2}^+$ transitions, the hindrance factor $B_{s.p.}/B_{exp}$ is given in the last column of Table II. Here, $B_{s.p.}$ has been evaluated for a neutron (proton) whenever the odd nucleus is reached by adding a neutron (proton) to the neighboring even-even

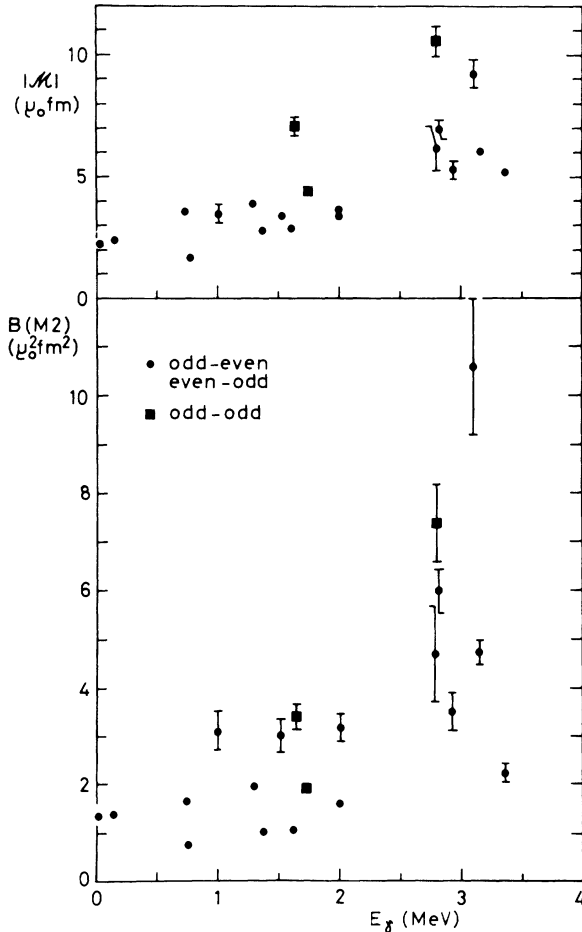


FIG. 6. Experimental $B(M2)$ values and reduced $M2$ matrix elements versus the transition energy E_γ .

nucleus. This choice corresponds to the sign of the respective $E3/M2$ mixing ratio which is determined by the sign of $g_s - \frac{2}{3} g_1$, and turned out to be positive (negative) for a neutron (proton) transition (see Table II).

C. Weak-coupling estimates

Kurath and Lawson⁷ have pointed out that the retardations of the $\frac{7}{2}^- \rightarrow \frac{3}{2}^+$ $M2$ transitions in ^{39,41}K and ^{39,41}Ca can be explained in terms of the Bansal-French-Zamick weak-coupling model¹⁰ as being mainly an isospin effect (apart from an additional inhibition due to quadrupole deformation). The 2.01 MeV $\frac{3}{2}^+$ state in ⁴¹Ca, for instance, is interpreted as a $(f_{7/2}^2 d_{3/2}^{-1})$ state with one additional $d_{3/2}$ neutron or proton excited to the $f_{7/2}$ orbit and the two $f_{7/2}$ nucleons coupled to $I_f = 0$, $T_f = 1$. A large part of the inhibition of the $M2$ ground state transition then follows quite naturally from a partial cancellation of the neutron and proton transition due to the different signs of their g factors.

The success of this simple model in predicting correct energies for the $\frac{7}{2}^-$ quasiparticle states and their analogs, $\frac{3}{2}^+$ quasihole states and stretched 7^+ two-quasiparticle states, has been stressed by several authors.^{31,32} We extended the weak-coupling approach to the states given in Table III and calculated the $M2$ transition energies and probabilities. The underlying idea of this model is based on the fact that the energy separation between the $T=0$ and $T=1$ ($f_{7/2} d_{3/2}^{-1}$) multiplets in ⁴⁰Ca is much larger than the splittings within each multiplet. The energy of an $(m p - k h)$ state is then given by

$$E(f^m d^{-k}) = E(f^m) - E(d^{-k}) + E_{int}, \quad (3)$$

where $E(f^m)$ denotes the (experimental) energy of the $f_{7/2}^m$ particle state and $E(d^{-k})$ the (experimental) energy of the $d_{3/2}^{-k}$ hole state. The particle-hole interaction $H_{int} = a + b(\vec{T}_f \cdot \vec{T}_d)$ produces an energy shift of

$$\begin{aligned}
E_{int} &= -amk + \frac{1}{2}b [T(T+1) - T_f(T_f+1) - T_d(T_d+1)] \\
&\quad + \frac{1}{4}c(m - 2T_{f3})(k + 2T_{d3}), \quad (4)
\end{aligned}$$

where the last term accounts for the Coulomb interaction between a proton and a proton hole. In our calculation we used the parameters $a = -0.25$ MeV, $b = +2.5$ MeV, and $c = -0.4$ MeV per proton which Bernstein³³ derived from the (2p-1h) spectrum in ⁴¹Ca and which are similar to the ones used by Bansal and French¹⁰ and by Zamick.¹¹ Recently, Sherr *et al.*³² proposed a slightly different set ($a = -0.25$ MeV, $b = +2.74$ MeV, and $c = -0.29$ MeV) from a fit to the $d_{3/2}$ proton hole states in the odd K and Sc isotopes.

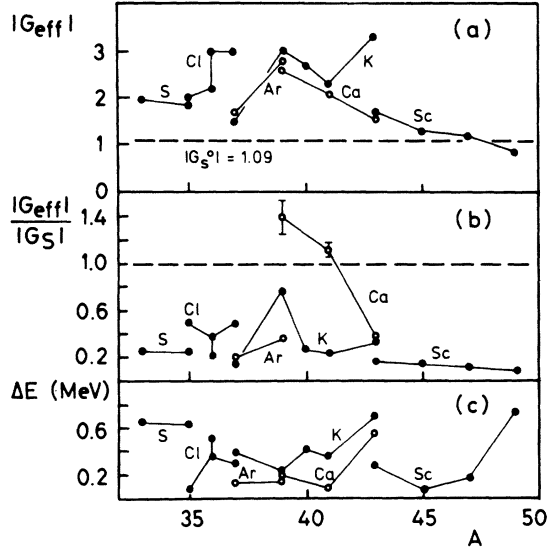


FIG. 7. (a) Effective $M2$ coupling constant $|G_{\text{eff}}|$ for all stretched $M2$ transitions in nuclei with $33 \leq A \leq 47$. (b) Ratios $|G_{\text{eff}}/G_S|$ of $M2$ transitions. The dashed line indicates the weak-coupling limit. (c) Difference between the experimental $M2$ transition energies and the corresponding weak-coupling estimates.

The calculated transition energies $E_{\text{BFZ}} = E(f^{m+1}d^{-k-1}) - E(f^m d^{-k})$ are given in Table III. We used the binding energies from the tables of Wapstra and Gove³⁴ and the energies, spins, and isospins of excited states from the compilation of Endt and Van der Leun.¹ Whenever several members of an isospin multiplet were known, the average value of E_{BFZ} is given in Table III. As can be seen from Table III and Fig. 7(c), the weak-coupling estimate is in fair agreement with the actual energy; the rms deviation is 300 keV. This also applies to the odd-odd nuclei ³⁶Cl and ⁴⁰K, where the predicted transition energies of 2.26 and 2.09 MeV (³⁶Cl) and 2.07 MeV (⁴⁰K) compare reasonably well with the experimental figures of 2.79, 1.73 and 1.65 MeV, respectively. Also included in Table III is the result of a similar calculation by Watson and Lee³¹ for the $\frac{7}{2}^-$ states in $33 \leq A \leq 41$ in which the constant b of the isospin term was replaced by the mass dependent isospin potential V_1/A with $V_1 = 102$ MeV.

The reduced transition probabilities $B_{\text{BFZ}}(M2)$ were calculated using the reduction technique of de Shalit and Talmi.³⁵ For the reduced matrix element of the transition

TABLE III. Weak-coupling estimates of transition energies and $B(M2)$ values.

Nucleus	f_T	Initial state			Final state			Transition energy			$B_{\text{BFZ}}/B_{\text{exp}}$	$ G_{\text{eff}} $	
		$(m+1)$	$I_f T_f; n I_d T_d; I$	$n I_d T_d; I$	m	$I_f T_f; (n+1)$	$I_d T_d; I'$	exp	BFZ	Watson-Lee			
³³ S	+1	1	$\frac{7}{2} \frac{1}{2}; 000;$	$\frac{7}{2}$	0	00;	1	$\frac{3}{2} \frac{1}{2}; \frac{3}{2}$	2.93	2.28	2.94	14.3 ± 2.0	2.03 ± 0.15
³⁵ S	+1	1	$\frac{7}{2} \frac{1}{2}; 201;$	$\frac{7}{2}$	0	00;	3	$\frac{3}{2} \frac{3}{2}; \frac{3}{2}$	1.99	1.37	1.93	16.4 ± 1.0	1.90 ± 0.06
³⁵ Cl	$-\frac{1}{3}$	1	$\frac{7}{2} \frac{1}{2}; 201;$	$\frac{7}{2}$	0	00;	3	$\frac{3}{2} \frac{1}{2}; \frac{3}{2}$	3.16	3.25	3.13	3.9 ± 0.3	2.04 ± 0.09
³⁶ Cl	-1	2	7 0; 201;	7	1	$\frac{7}{2} \frac{1}{2};$	3	$\frac{3}{2} \frac{1}{2}; 5$	2.79	2.26	...	9.9 ± 1.2	2.36 ± 0.12
³⁶ Cl	+1	1	$\frac{7}{2} \frac{1}{2}; 3 \frac{3}{2} \frac{1}{2};$	5	0	00;	4	3 1; 3	1.73	2.09	...	6.7 ± 0.3	2.95 ± 0.07
³⁷ Cl	$-\frac{3}{5}$	1	$\frac{7}{2} \frac{1}{2}; 402;$	$\frac{7}{2}$	0	00;	5	$\frac{3}{2} \frac{3}{2}; \frac{3}{2}$	3.10	3.40	3.10	4.4 ± 0.6	3.0 ± 0.2
³⁷ Ar	+1	1	$\frac{7}{2} \frac{1}{2}; 400;$	$\frac{7}{2}$	0	00;	5	$\frac{3}{2} \frac{1}{2}; \frac{3}{2}$	1.61	1.42	1.59	25.5 ± 0.5	1.52 ± 0.01
³⁷ K	-1	1	$\frac{7}{2} \frac{1}{2}; 400;$	$\frac{7}{2}$	0	00;	5	$\frac{3}{2} \frac{1}{2}; \frac{3}{2}$	1.37	0.97	1.44	44.6 ± 2.2	1.47 ± 0.04
³⁹ Ar	+1	2	0 1; 5 $\frac{3}{2} \frac{1}{2};$	$\frac{3}{2}$	1	$\frac{7}{2} \frac{1}{2};$	6	0 1; $\frac{7}{2}$	1.52	1.37	...	7.8 ± 0.4	2.75 ± 0.07
³⁹ K	$-\frac{1}{3}$	1	$\frac{7}{2} \frac{1}{2}; 601;$	$\frac{7}{2}$	0	00;	7	$\frac{3}{2} \frac{1}{2}; \frac{3}{2}$	2.81	2.61	2.82	1.9 ± 0.2	2.86 ± 0.15
³⁹ Ca	$+\frac{1}{3}$	1	$\frac{7}{2} \frac{1}{2}; 601;$	$\frac{7}{2}$	0	00;	7	$\frac{3}{2} \frac{1}{2}; \frac{3}{2}$	2.79	2.59	2.40	0.5 ± 0.1	2.6 ± 0.3
⁴⁰ K	-1	2	7 0; 601;	7	1	$\frac{7}{2} \frac{1}{2};$	7	$\frac{3}{2} \frac{1}{2}; 5$	1.65	2.07	...	13.8 ± 0.8	2.65 ± 0.07
⁴¹ K	-1	3	$\frac{7}{2} \frac{1}{2}; 601;$	$\frac{7}{2}$	2	01;	7	$\frac{3}{2} \frac{1}{2}; \frac{3}{2}$	1.29	1.65	...	18.9 ± 1.0	2.26 ± 0.06
⁴¹ Ca	$+\frac{1}{3}$	2	0 1; 7 $\frac{3}{2} \frac{1}{2};$	$\frac{3}{2}$	1	$\frac{7}{2} \frac{1}{2};$	8	0 0; $\frac{7}{2}$	2.01	1.92	...	0.8 ± 0.1	2.05 ± 0.10
⁴¹ Ca	+1	2	7 0; 7 $\frac{3}{2} \frac{1}{2};$	$\frac{3}{2}$	1	$\frac{7}{2} \frac{1}{2};$	8	0 0; $\frac{7}{2}$	3.37	4.79	...	53 ± 4	1.35 ± 0.06
⁴³ K	-1	5	$\frac{7}{2} \frac{3}{2}; 601;$	$\frac{7}{2}$	4	02;	7	$\frac{3}{2} \frac{1}{2}; \frac{3}{2}$	0.74	1.44	...	9.1 ± 0.4	3.27 ± 0.08
⁴³ Ca	$+\frac{3}{5}$	4	0 2; 7 $\frac{3}{2} \frac{1}{2};$	$\frac{3}{2}$	3	$\frac{7}{2} \frac{3}{2};$	8	0 0; $\frac{7}{2}$	0.99	1.55	...	7.1 ± 0.9	1.56 ± 0.10
⁴³ Sc	-1	4	0 0; 3 $\frac{1}{2} \frac{3}{2};$	$\frac{3}{2}$	3	$\frac{7}{2} \frac{1}{2};$	8	0 0; $\frac{7}{2}$	0.15	-0.13	...	33.6 ± 0.4	1.70 ± 0.01
⁴⁵ Sc	-1	6	0 1; 7 $\frac{3}{2} \frac{1}{2};$	$\frac{3}{2}$	5	$\frac{7}{2} \frac{3}{2};$	8	0 0; $\frac{7}{2}$	0.01	-0.07	...	56 ± 3	1.32 ± 0.03
⁴⁷ Sc	-1	8	0 2; 7 $\frac{3}{2} \frac{1}{2};$	$\frac{3}{2}$	7	$\frac{7}{2} \frac{3}{2};$	8	0 0; $\frac{7}{2}$	0.76	0.58	...	73 ± 11	1.15 ± 0.09

$$[f^{m+1}(I_f T_f) d^n(I_d T_d)]_{IT} \rightarrow [f^m(I'_f T'_f) d^{n+1}(I'_d T'_d)]_{I'T'=T}$$

one obtains the expression

$$\begin{aligned} \mathfrak{M}_{\text{BFZ}} &= \langle f^m d^{n+1} \| M2 \| f^{m+1} d^n \rangle \\ &= \left(\frac{18}{7\pi} \right)^{1/2} \langle \tau \rangle \mu_0 [(m+1)(n+1)]^{1/2} \sum a a' (-)^q C_d C_f (G^0 - f_T G^1) \hat{I}' \hat{T}'_d \hat{T}'_f \hat{I}'_d \hat{I}'_f \begin{Bmatrix} T'_d & T'_f & T \\ T_f & T_d & \frac{1}{2} \end{Bmatrix} \begin{Bmatrix} I'_d & I'_f & I' \\ I_d & I_f & I \\ \frac{3}{2} & \frac{7}{2} & 2 \end{Bmatrix}, \end{aligned} \quad (5)$$

where $\hat{I} \equiv (2I+1)^{1/2}$ and $q = T + 2T'_f + T_d - T_f + I'_f - I_f + m + \frac{1}{2}$. The quantities C_d and C_f are c.f.p. (Ref. 35), and a and a' are the amplitudes of the particular initial and final configurations considered; they are unity in the extreme weak-coupling picture (lowest seniority). The isoscalar and isovector coupling constants G^0 and G^1 are defined as

$$\begin{aligned} G^0 &= \frac{2}{3}(g_1^p + g_1^n) - (g_s^p + g_s^n), \\ G^1 &= \frac{2}{3}(g_1^p - g_1^n) - (g_s^p - g_s^n). \end{aligned} \quad (6)$$

Finally, the quantity

$$f_T = \frac{T_3}{T(T+1)} [T'_d(T'_d+1) - T_d(T_d+1) + T_f(T_f+1) - T'_f(T'_f+1)] \quad (7)$$

varies between $f_T = +1$ (pure neutron transition) and $f_T = -1$ (single-proton transition).

The ratios $B_{\text{BFZ}}/B_{\text{exp}}$ calculated in the extreme weak-coupling model (lowest seniority: $a = a' = 1$) using free nucleon g factors ($G_S^0 = -1.09$, $G_S^1 = -8.75$) are given in Table III. As mentioned before, the transitions in ^{39}K , ^{39}Ca , and ^{41}Ca are reproduced reasonably well, but in the other cases a further reduction of $B(M2)$ by as much as a factor of 70 is needed. Another failure of the weak-coupling model concerns the mirror transitions in ^{37}Ar and ^{37}K as well as in ^{39}K and ^{39}Ca . For each pair of mirror transitions, the experimental $B(M2)$ values are equal whereas the weak-coupling model predicts a ratio of 1.7 ($A = 37$) and 4.8 ($A = 39$) between them.

D. Effective $M2$ coupling constants

By using the lowest seniority BFZ wave functions, one neglects the recoupling of equivalent particles to different spin-isospin combinations ($I_d T_d$; $I_f T_f$) as well as the influence of orbits further away from the Fermi level. Although we are not aware of a shell model calculation for the non-normal-parity states in the Ca region using the full $\{2s1d1f2p\}$ model space, several attempts have been made to trace the origin of the systematic $M2$ hindrance.

Lawson and Macfarlane⁸ discussed the $\frac{3}{2}^+ - \frac{7}{2}^-$ $M2$ transitions in the Sc isotopes in terms of the

strong-coupling model. They showed that the deformation of the effective single-particle potential leads to considerable $I_f = 2^+$ core-excitation amplitude in the wave function of the $d_{3/2}$ hole states. To a large extent this component cancels the BFZ $I_f = 0^+$ contribution. Harris and collaborators¹² stressed the effect of a similar $I_d = 2^+$ core-excitation component in the wave functions of the $\frac{7}{2}^-$ states in ^{35}S , ^{35}Cl , and ^{37}Cl . Instead of *one* large core-excitation component within the $\{d_{3/2}f_{7/2}\}$ model space, many coherently acting small components may produce the inhibition of the transition matrix element. Using first-order perturbation theory within the full $\{2s1d1f2p\}$ model space, Towner *et al.*⁹ found that the repulsive $T = 1$ interaction between the $f_{7/2}$ particle and the $d_{3/2}$ hole is responsible for the hindrance of the $1f_{7/2} \rightarrow 1d_{3/2}$ first-forbidden β decays around ^{40}Ca . As the operators for radiative $M2$ and first-forbidden β transitions are essentially the same, one may infer this explanation also for the $1f_{7/2} \rightarrow 1d_{3/2}$ $M2$ transitions.

As this inhibition turned out to be rather independent of the particular nucleus, one may retain the zeroth-order BFZ model wave functions and introduce the effective $M2$ coupling constant G_{eff} ,

$$G_{\text{eff}} = G_S [B_{\text{exp}}(M2)/B_{\text{BFZ}}(M2)]^{1/2}, \quad (8)$$

where G_S has been defined as $G_S = G_S^0 - f_T G_S^1$. The values of $|G_{\text{eff}}|$ are given in the last column of Table III and are plotted in Fig. 7(a) versus the mass number A ; they are distributed around $G_{\text{eff}} = 2.1$ with a FWHM of $\Delta G_{\text{eff}} = 0.6$.

It is interesting to note that G_{eff} does not depend on the isospin factor f_T , which is proportional to T_3 . Indeed, the average value $\overline{G_{\text{eff}}(n)} = 2.1$ for the neutron transitions ($f_T = +1$) compares well with the respective average value $\overline{G_{\text{eff}}(p)} = 2.0$ for the proton transitions ($f_T = -1$). This points again to a strong reduction of the isovector coupling constant G^1 with respect to the free nucleon value $G_S^1 = -8.75$. In Fig. 8 we have plotted the ratio $|G_{\text{eff}}/G_S|$ versus the isospin factor f_T . From the 14 stretched $M2$ transitions with $|f_T| = 1$ listed in Table III one finds $|G_{\text{eff}}/G_S| = 0.24 \pm 0.06$, in good agreement with the result $G_{\text{eff}}/G_S \approx 0.25$ de-

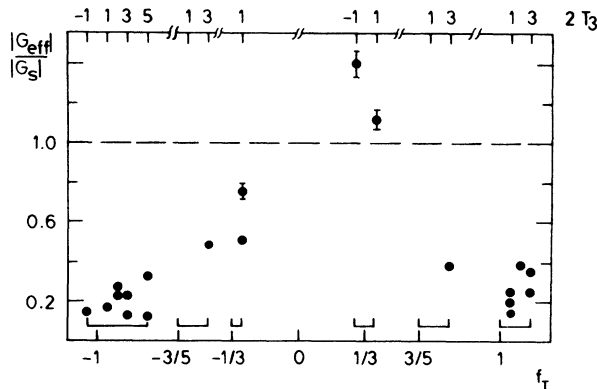


FIG. 8. Ratio $|G_{\text{eff}}/G_S|$ versus the isospin factor f_T defined in Eq. (7). The dashed line indicates again the weak-coupling limit. Values at $f_T = +1$ (-1) correspond to single-neutron (proton) transitions.

duced by Ejiri *et al.*¹⁴ for the $1h_{11/2} \rightarrow 1g_{7/2}$ quasi-particle $M2$ transitions. The six cases with $|f_T| < 1$, on the other hand, show a clear tendency of $|G_{\text{eff}}/G_S|$ increasing for $f_T \rightarrow 0$. This trend again indicates the strong reduction of the isovector part G^1 , whereas the isoscalar part G^0 seems to be close to the free nucleon value.

IV. CONCLUSION

The experimental information on stretched $M2$ transitions in the $A = 40$ region has been updated by performing recoil distance lifetime measurements in $^{35,36}\text{Cl}$, ^{40}K , and ^{41}Ca . The reduced matrix elements of the 20 known $M2$ transitions associated with the decay of a nucleon from the $1f_{7/2}$ orbit to the $1d_{3/2}$ orbit have been discussed in terms of the Bansal-French-Zamick model. An overall reduction of the $M2$ coupling constant $G_{\text{eff}}/G_S = 0.24 \pm 0.06$ with respect to the single-particle estimate has been deduced for transitions with $|f_T| = 1$. Similar inhibitions had been previously observed for $M2$ transitions in heavy nuclei¹⁴ as well as for the first-forbidden β decays⁹ around ^{40}Ca and had been traced to the repulsive $T = 1$ particle-hole interaction. We finally note the observation of a correlation between the reduced $M2$ matrix element and the transition energy.

The authors are indebted to Dr. F. Brandolini, Dr. H. Ejiri, and Dr. R. D. Lawson for fruitful discussions; to Mr. N. Möllers for assistance during the measurement; and to Mrs. B. Bohnhoff for the target preparation.

*Supported by Bundesministerium für Forschung und Technologie.

†Permanent address: Department of Physics, University of Helsinki, Finland.

‡Present address: Kernforschungsanlage Jülich, Germany.

¹P. M. Endt and C. van der Leun, Nucl. Phys. **A214**, 1 (1973).

²R. E. Holland, F. J. Lynch, and K. E. Nysten, Phys. Rev. Lett. **13**, 241 (1964).

³A. Graue, L. H. Herland, J. R. Lien, G. E. Sandvik, E. R. Cosman, and W. H. Moore, Nucl. Phys. **A136**, 577 (1969); A. R. Morrison, *ibid.* **A140**, 97 (1970); J. G. van der Baan and H. G. Leighton, *ibid.* **A170**, 607 (1971).

⁴M. C. Mermaz, C. A. Whitten, J. W. Champlin, A. J. Howard, and D. A. Bromley, Phys. Rev. C **4**, 1778 (1971); S. Sen, C. L. Hollas, and P. J. Riley, *ibid.* **3**, 2314 (1971); M. Hagen, U. Janetzki, K. H. Maier, and H. Fuchs, Nucl. Phys. **A152**, 404 (1970).

⁵U. Lynen, R. Santo, D. Schmitt, and R. Stock, Phys. Lett. **27B**, 76 (1968); R. Santo, R. Stock, J. H. Bjerregard, O. Hansen, O. Nathan, R. Chapman, and S. Hinds, Nucl. Phys. **A118**, 409 (1968).

⁶E. Rivet, R. H. Pehl, J. Cerny, and B. G. Harvey, Phys. Rev. **141**, 1021 (1965); R. Kouzes and R. Sherr, Bull. Am. Phys. Soc. **18**, 602 (1973).

⁷D. Kurath and R. D. Lawson, Phys. Rev. **161**, 915 (1967).

⁸R. D. Lawson and M. H. Macfarlane, Phys. Rev. Lett. **14**, 152 (1965).

⁹I. S. Towner, E. K. Warburton, and G. T. Garvey, Ann.

Phys. (N.Y.) **66**, 674 (1971).

¹⁰R. K. Bansal and J. B. French, Phys. Lett. **11**, 145 (1964).

¹¹L. Zamick, Phys. Lett. **19**, 580 (1965).

¹²F. C. Erne, Nucl. Phys. **84**, 91 (1966); S. Maripuu, Nucl. Phys. **A123**, 357 (1969); S. Maripuu and G. A. Hocken, *ibid.* **A141**, 481 (1970); G. I. Harris and J. J. Perizzo, Phys. Rev. C **2**, 1347 (1970).

¹³B. H. Wildenthal (unpublished).

¹⁴H. Ejiri, T. Shibata, and M. Fujiwara, Phys. Rev. C **8**, 1892 (1973); H. Ejiri, T. Shibata, and K. Satoh, Phys. Lett. **38B**, 73 (1972).

¹⁵R. E. Lynch and F. J. Holland, Phys. Rev. **114**, 825 (1959).

¹⁶J. Dauk, Doctoral thesis, Köln, 1974 (unpublished).

¹⁷P. J. Nolan, P. A. Butler, P. E. Garr, L. L. Gadeken, A. N. James, J. F. Sharpey-Schafer, and D. A. Viggars, J. Phys. **A6**, L37 (1973) and unpublished work.

¹⁸J. W. Olness, A. H. Lumpkin, J. J. Kolata, E. K. Warburton, J. S. Kim, and Y. K. Lee, Phys. Rev. C **11**, 110 (1975).

¹⁹K. P. Lieb, M. Uhrmacher, J. Dauk, and A. M. Kleinfeld, Nucl. Phys. **A223**, 445 (1974).

²⁰T. K. Alexander, and A. Bell, Nucl. Instrum. Methods **81**, 22 (1970).

²¹H. G. Friederichs, A. Gelberg, B. Heits, K. P. Lieb, M. Uhrmacher, K. O. Zell, and P. von Brentano, Phys. Rev. Lett. **34**, 745 (1975); M. Uhrmacher, Diplom thesis, Köln, 1973 (unpublished).

²²P. R. Lornie, E. M. Jayasinghe, G. D. Jones, H. G. Price, M. F. Thomas, D. J. Twin, and P. J. Nolan,

- J. Phys. A7, 1977 (1974).
- ²³R. Rascher, K. P. Lieb, and M. Uhrmacher, Phys. Rev. C 13, 1217 (1976).
- ²⁴M. Uhrmacher, J. Dauk, N. Wüst, K. P. Lieb, and A. M. Kleinfeld, Z. Phys. A272, 403 (1975).
- ²⁵J. C. Merdinger, and W. Dehnhardt, J. Phys. 33, 110 (1972).
- ²⁶W. Kessel, R. Bass, E. C. Hagen, N. R. Roberson, C. R. Gould, and D. R. Tilley, Nucl. Phys. A223, 253 (1974).
- ²⁷J. Dauk, K. P. Lieb, and A. M. Kleinfeld, Nucl. Phys. A241, 170 (1975).
- ²⁸B. E. Cooke, R. I. Kozub, W. McLatchie, T. K. Alexander, J. S. Forster, C. Broude, and J. R. Beene, J. Phys. G2, 131 (1976).
- ²⁹F. Brandolini, M. de Poli, and C. Rossi-Alvarez, Lett. Nuovo Cimento 8, 342 (1973).
- ³⁰A. Bohr, and B. R. Mottelson, *Nuclear Structure* (Benjamin, New York, 1969), Vol. I, p. 388.
- ³¹D. D. Watson and F. D. Lee, Phys. Lett. 25B, 472 (1967).
- ³²R. Sherr, R. Kouzes, and R. DelVecchio, Phys. Lett. 52B, 401 (1974); R. Sherr, and G. Bertsch, Phys. Rev. C 12, 1671 (1975).
- ³³A. M. Bernstein, Ann. Phys. (N.Y.) 69, 19 (1972).
- ³⁴A. H. Wapstra, and N. B. Gover, Nucl. Data A 9, 265 (1971).
- ³⁵A. de Shalit, and I. Talmi, *Nuclear Shell Theory* (Academic, London, 1963).
- ³⁶F. Ingebretsen, T. K. Alexander, O. Häusser, and D. Pelte, Can. J. Phys. 47, 1295 (1969).
- ³⁷R. D. Barton, J. S. Wadden, A. L. Carter, and H. L. Pai, Can. J. Phys. 49, 971 (1971).
- ³⁸N. Anyas-Weiss, R. Griffiths, N. A. Jelley, W. Randolph, J. Szücs, and T. K. Alexander, Nucl. Phys. A201, 513 (1973).
- ³⁹M. A. Van Driel, H. H. Eggenhuisen, J. A. J. Hermans, D. Bucurescu, H. A. van Rinsvelt, and G. A. P. Engelbertink, Nucl. Phys. A226, 326 (1974).
- ⁴⁰M. J. Verucci *et al.*, Can. J. Phys. 51, 1039 (1973).
- ⁴¹J. J. Kolata, P. Gorodetzky, J. W. Olness, A. R. Poletti, and E. K. Warburton, Phys. Rev. C 9, 953 (1974); P. D. Bond and B. D. Kern, *ibid.* 6, 873 (1972); W. Kessel, R. Bass, and R. Wechsung, Nucl. Phys. A206, 193 (1972).
- ⁴²P. Gorodetzky, J. J. Kolata, J. W. Olness, A. R. Poletti, and E. K. Warburton, Phys. Rev. Lett. 31, 1067 (1973).
- ⁴³E. Bozek, C. Gehringer, C. Jaeger, and J. C. Merdinger, Nucl. Phys. A250, 257 (1975).
- ⁴⁴P. J. Nolan (private communication).
- ⁴⁵M. F. Thomas, C. K. Davis, G. D. Lones, H. G. Price, and P. J. Twin, J. Phys. A7, 1985 (1974).
- ⁴⁶P. J. Nolan, L. L. Gadeken, A. J. Brown, P. A. Butler, L. L. Green, A. N. James, J. F. Sharpey-Schafer, and D. A. Viggars, J. Phys. A7, 1437 (1975).